Journal of Alloys and Compounds 499 (2010) 30–34

Contents lists available at ScienceDirect

Journal of Alloys and Compounds

journal homepage: www.elsevier.com/locate/jallcom

Porous and superparamagnetic magnesium ferrite film fabricated via a precursor route

Xu Xiang, Guoli Fan, Jun Fan, Feng Li*

State Key Laboratory of Chemical Resource Engineering, Beijing University of Chemical Technology, P.O. Box 98, Beijing, 100029, PR China

ARTICLE INFO

Article history:
Received 1 December 2009
Received in revised form 6 March 2010
Accepted 14 March 2010
Available online 19 March 2010

Keywords:
Inorganic materials
Magnetic films and multilayers
Chemical synthesis
Microstructure

ABSTRACT

Porous magnesium ferrite film was fabricated via a single-source precursor strategy involving thermal conversion of $Mg^{(II)}Fe^{(III)}$-layered double hydroxide (MgFe-LDH) precursor film formed in situ on sulfonated silicon substrate, followed by selective etching of excessive MgO phase in the calcined precursor film. XRD and EDS analyses confirm the formation of single phase $MgFe_2O_4$ after etching of MgO. The as-formed $MgFe_2O_4$ film exhibits porous and particulate structure consisting of fused particle aggregates. AFM observation reveals the rough surface nature of the ferrite film. The magnetic characterization shows the enhanced saturation magnetization of $MgFe_2O_4$ film (c.a. 37.1 emu/g), compared to that of $MgFe_2O_4$ powder synthesized by a conventional solid-state reaction. Importantly, the temperature-dependent magnetization of $MgFe_2O_4$ film exhibits unusual superparamagnetic characteristic. In addition, the film modified with organic molecule shows superhydrophobicity. Such significant magnetic and interfacial property of ferrite film can open up new opportunities for advanced applications of this material.

1. Introduction

Spinel-type ferrites are currently intriguing materials due to their promising applications in a variety of fields such as ferrofluid, magnetic storage, medical and bio-inspired technology [1–6]. Among them, magnesium ferrite ($MgFe_2O_4$) known as a ferrimagnetic material has been widely envisaged, stemming from its essentially magnetic and electronic properties. It is known that the magnetic properties of ferrites are extremely sensitive to both their chemical compositions (i.e. substitution of cations) and microstructure (i.e. particle size, shape and porosity), which strongly depends on the preparation methods [7–9]. The structure-dependent magnetism of ferrites is of critical significance not only for exploring the fundamental physical phenomenon of magnetic materials but also for developing new magnetic devices in various practical fields. However, studies on porous ferrite thin films with unique texture are scarce. Therefore, it is highly desirable to develop synthesis methods of ferrite films with porous microstructure for achieving structure-associated physicochemical properties.

Layered double hydroxides (LDHs) are known to be synthetic anionic clays with a hydrotalcite-like layered structure. The divalent cations in the layers are partly substituted by the trivalent cations, giving positively charged layers with charge-balancing anions intercalated into the interlayer galleries [10,11]. LDHs have a broad range of applications as catalytic materials, absorption, additives in polymers and in medicine and functional devices [12–15]. Especially, LDHs are potential precursors for obtaining mixed-metal oxides like spinel ferrites since the calcination of LDHs at a given temperature leads to spinel phases [16]. However, the products are commonly mixed with the metal oxides and/or spinels because of the abundant of divalent cations in LDH precursors, i.e. the ratio of M^{2+}/M^{3+} in LDH is larger than their stoichiometry in ferrites (usually $M^{2+}/M^{3+} = 0.5$). Our previous research revealed that the chemically pure spinel ferrites nanoparticles or monoliths could be synthesized from LDH precursors [17–19]. The ferrite films on plane substrates, however, have not been fabricated via a precursor route.

In this paper, we attempt to prepare ferrite films with a two-dimensional condensed state via an innovative single-source precursor synthesis strategy from LDH. The strategy involved the in situ growth of MgFe-LDH precursor film over a sulfonated silicon substrate, and subsequently the calcination and etching steps of precursor film. The resultant ferrite film exhibits porous and particulate morphology due to the removal of resulting MgO phase. The film shows distinctly magnetic and surface properties owing to the nature of structure.

2. Experimental

2.1. Sulfonation of silicon substrate

The commercially available Si wafer was cleaned in an ultrasonic bath with acetone, ethanol and deionized water, respectively, and subsequently dried in N_2 atmosphere for further use. The cleaned Si substrate was subject to surface sul-

* Corresponding author. Tel.: +86 10 64451226; fax: +86 10 64425385.
E-mail address: lifeng_70@163.com (F. Li).

0925-8388/$ – see front matter © 2010 Elsevier B.V. All rights reserved.
doi:10.1016/j.jallcom.2010.03.125

fonated by dipping into concentrated sulfuric acid solution (98% in wt) for 5 days at room temperature. Afterwards, the substrate was thoroughly washed with large amount of deionized water to remove adsorbed species of surface and dried at 60 °C for 12 h.

2.2. Preparation of MgFe-LDH precursor film

The analytical grade $Mg(NO_3)_2{\cdot}6H_2O$ and $Fe(NO_3)_3{\cdot}9H_2O$ with Mg^{2+}/Fe^{3+} molar ratio of 3.0 (total concentration of 1.2 mol l^{-1}) were dissolved in deionized water to form mixed salt solution. The sulfonated Si substrate was firstly soaked in the solution for 2 h. The salt solution was titrated with a mixed alkali solution of NaOH ($[OH^-] = 1.6([Mg^{2+}] + [Fe^{3+}])$) and Na_2CO_3 ($[CO_3{}^{2-}] = 2[Fe^{3+}]$) under magnetic stirring at room temperature till pH 10.5. Subsequently, the resulting slurry and Si substrate was transferred into a Teflon-lined autoclave (100 ml volume), which was sealed and held in an oven at 160 °C for 24 h. Finally, MgFe-LDH film was grown on the surface of sulfonated Si substrate.

2.3. Fabrication of $MgFe_2O_4$ film

The as-prepared MgFe-LDH film was thermally treated in a muffle furnace at 900 °C for 3 h to form $MgFe_2O_4$-MgO mixed oxide film. For obtaining the $MgFe_2O_4$ film, the mixed oxide film was carefully immersed into an aqueous solution of $(NH_4)_2SO_4$ (10 wt%) and maintained at 70 °C for a period of 48 h. Afterwards, the film was thoroughly washed with deionized water to remove the absorbed species and then dried at 70 °C for more than 8 h.

2.4. Characterization

Powder X-ray diffraction (XRD) was achieved at room temperature on Shimadzu XRD-6000 diffractometer (graphite-filtered Cu Kα, λ = 0.15418 nm, 40 kV, 30 mA). Signals were collected at a scan speed of 4°/min.

The morphology and compositions of samples were characterized by scanning electron microscopy (SEM) on a Hitachi S4700 microscopy equipped with energy dispersive X-ray spectroscopy (EDS, Oxford Instrument).

X-ray photoelectron spectra (XPS) were recorded on a Thermo VG ESCALAB250 X-ray photoelectron spectrometer at a base pressure of 2×10^{-9} Pa using Al Kα X-ray as the excitation source. The binding energy (BE) calibration of spectra was referenced to C 1s spectrum at 284.8 eV.

Scanning probe microscopy was carried out on a Nanoscope IIIa MultiMode SPM (Veeco Instruments, Santa Barbara, CA) in tapping mode under ambient conditions. Roughness data were obtained by using atomic force microscopy (AFM) software (Digital Instruments, Version 6.12).

Magnetization of samples was measured at room temperature on a local-made JDM-13 vibrating sample magnetometer (VSM). Temperature- and field-dependence magnetization of samples was measured on a Quantum Design MPMS-XL superconducting quantum interference device (SQUID). The magnetic hysteresis loops were obtained after cooling the sample to measurement temperatures in zero-field and then increasing the field from 0 to 1 T. The magnetization was measured in zero-field cooling (ZFC) and field cooling (FC) modes in the temperature range 5–300 K and with an applied field of 100 Oe.

Water contact angles (CA) on the ferrite films were measured with a sessile drop (5 μl) at three different points of each sample by using a commercial drop-shape analysis system (DSA100, KRüSS GmbH, Germany) at ambient temperature. Before the measurement, the surfaces of films were modified by n-octadecanoic acid.

3. Results and discussion

As shown in Fig. 1a, the XRD pattern of as-deposited MgFe-LDH powder scraped from substrate presents the characteristic reflections of hydrotalcite-like materials i.e. (0 0 3), (0 0 6), and (0 1 2), indicative of the formation of a single LDH phase [11]. The XPS analysis indicates the existence of C, O, S and Si elements on silicon substrate (no shown), and the S 2p spectrum shows a binding energy (B.E.) of 168.8 eV, corresponding to the bonding of sulfur in sulfonate. The XPS result confirms the grafting of sulfonate groups onto the surface of silicon substrate after sulfonation. As a result, the sulfonation provides abundant anionic sulfonate groups on substrate surface, leading to strong adhesion of resulting LDH to the substrate and dense growth of LDH crystallites under hydrothermal conditions.

After calcined at 900 °C, the layered structure of LDH disappears and new reflections appear, which can be assigned to cubic MgO and spinel-type $MgFe_2O_4$ phases (Fig. 1b). The formation of MgO is attributed to the abundance of Mg^{2+} cations in the precursor with a Mg^{2+}/Fe^{3+} ratio of 3. After the etching of self-generated MgO phase,

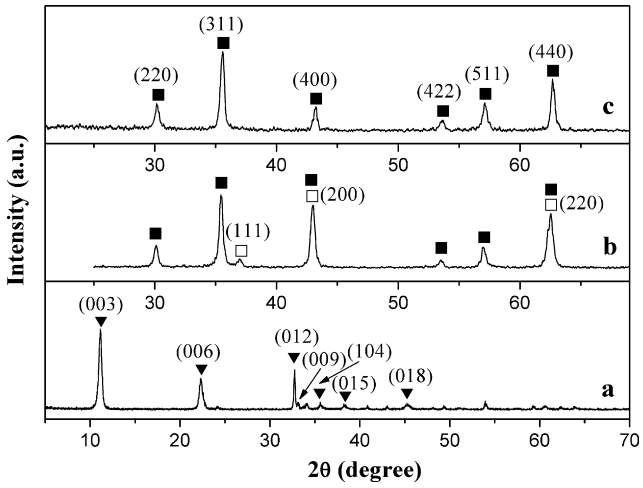

Fig. 1. XRD patterns of as-deposited MgFe-LDH (a), MgFe-LDH after calcination at 900 °C (b), and the calcined MgFe-LDH after the removal of MgO by the selective etching (c). (Triangle denotes LDH, solid square denotes $MgFe_2O_4$ and hollow square denotes MgO.)

the pattern of resultant shows typical reflections of spinel phase (Fig. 1c). It is noteworthy that the reflection (Fig. 1b) corresponding to plane (1 1 1) of MgO disappears after the selective etching of MgO in a weak acidic aqueous solution, while the relative intensity of reflection at $2\theta = 42.9°$ apparently decreases in the corresponding angle of Fig. 1c, owing to the effective removal of MgO phase. From the value of full-width at half-maximum (FWHM) of the reflection by using Scherrer equation [$L = 0.89\lambda/\beta(\theta)\cos\theta$], where L is the crystallite size, λ is the wavelength of the radiation used (0.15418 nm), θ is the Bragg reflection angle, and $\beta(\theta)$ is the FWHM of the reflections, the crystallite size of resultant ferrite is calculated to be c.a. 24 nm from the strongest reflection (3 1 1).

Fig. 2a and b shows SEM images of MgFe-LDH film on substrate. It is interestingly noted that the LDH plates almost upstandingly grow with a axis perpendicular to the substrate. The vertical orientation growth of LDH may be due to the hydrophilicity of sulfonate groups grafted to the substrate, thus leading to the affinity between the surfaces of resulting LDH and the sulfonate groups. Furthermore, one can see that these standing plates connect each other and form a nest-like surface morphology. The cross-section observation reveals the thickness of the film reaches c.a. 5 μm (Fig. 2c).

After calcination, MgFe-LDH precursor film lost the interconnected plate-like morphology and transformed into a continuous film with roughly particulate appearance owing to the collapse of LDH layers and the formation of new MgO and $MgFe_2O_4$ phases (Fig. 3a). A large amount of irregular particles extrude from the surface of film owing to the phase segregation of MgO and ferrite upon calcination. No observable porous structure is formed in this stage. Due to the fact that MgO phase accounts for the majority in calcined MgFe-LDH film (theoretically 75% in molar percentage) and acts as a dispersing matrix in the composite film, one can see from Fig. 3b and c that the resultant $MgFe_2O_4$ film shows a porous and sub-spherical particulate morphology after the selective etching of MgO. The particle sizes of ferrite observed are much larger than that calculated from FWHM value of reflection by Scherrer equation, which demonstrates that the $MgFe_2O_4$ particles formed here are kind of aggregates of multi-crystallite. The coalescence and fuse behaviours among crystallites or grains occur during the etching. The complete etching of self-generated MgO phase is also determined by EDS analysis (Fig. 3d). Quantitative analysis shows that Mg/Fe atomic ratio is 0.55, close to stoichiometry of ferrite. The above characterization confirms that the $MgFe_2O_4$ ferrite film is formed after the etching of MgO.

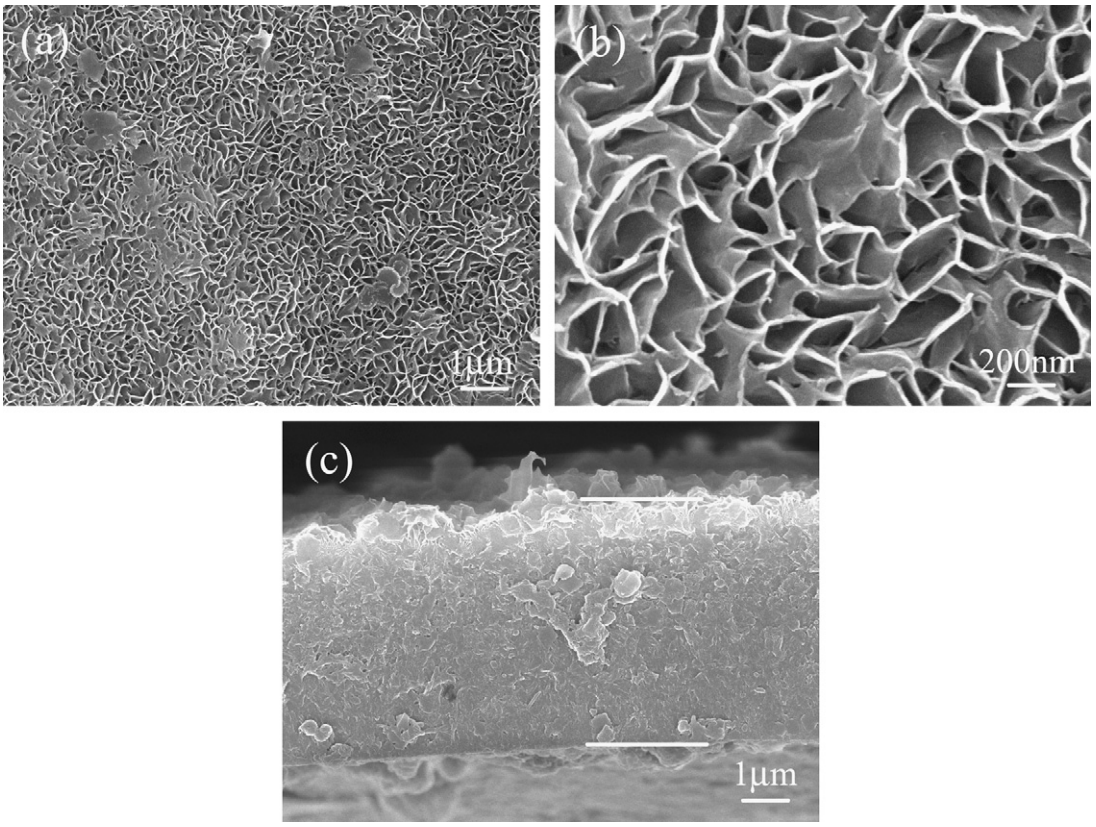

Fig. 2. SEM images of MgFe-LDH film (a) and (b), cross-section image of MgFe-LDH film (c).

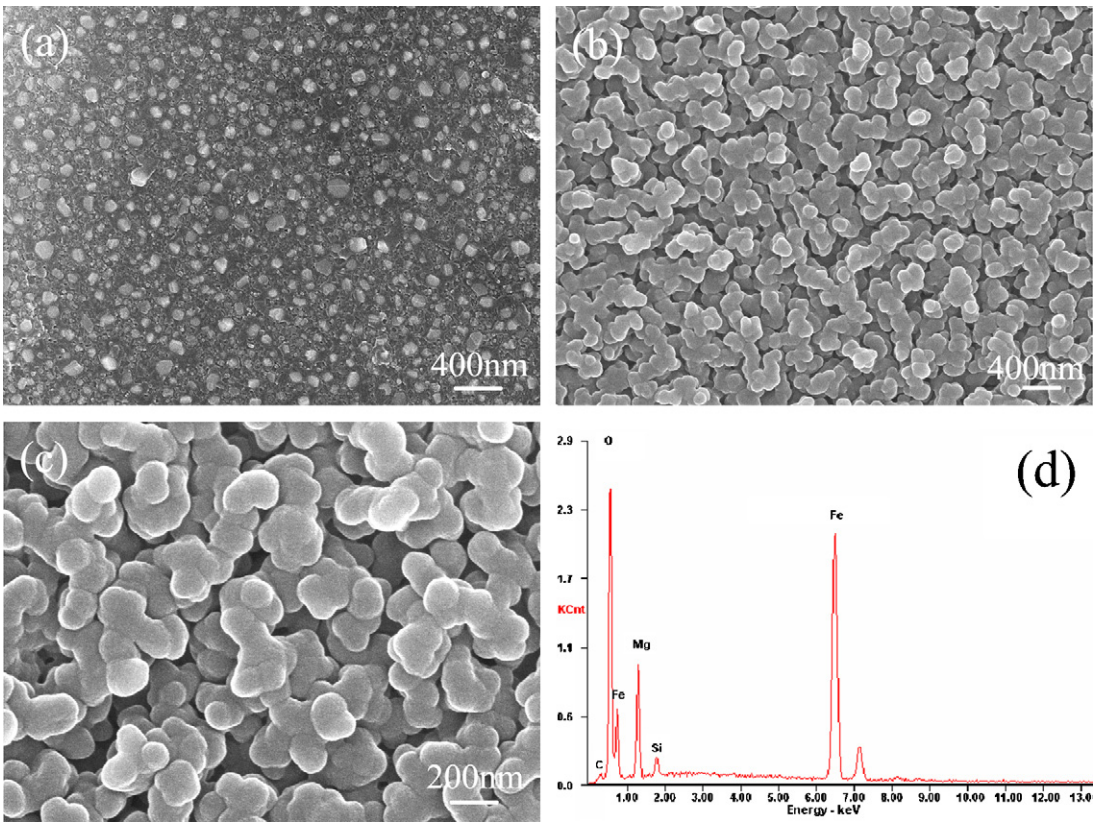

Fig. 3. SEM images of calcined MgFe-LDH film at 900 °C (a), $MgFe_2O_4$ film after the selective etching of MgO (b and c) and EDX spectrum of the $MgFe_2O_4$ ferrite film (d).

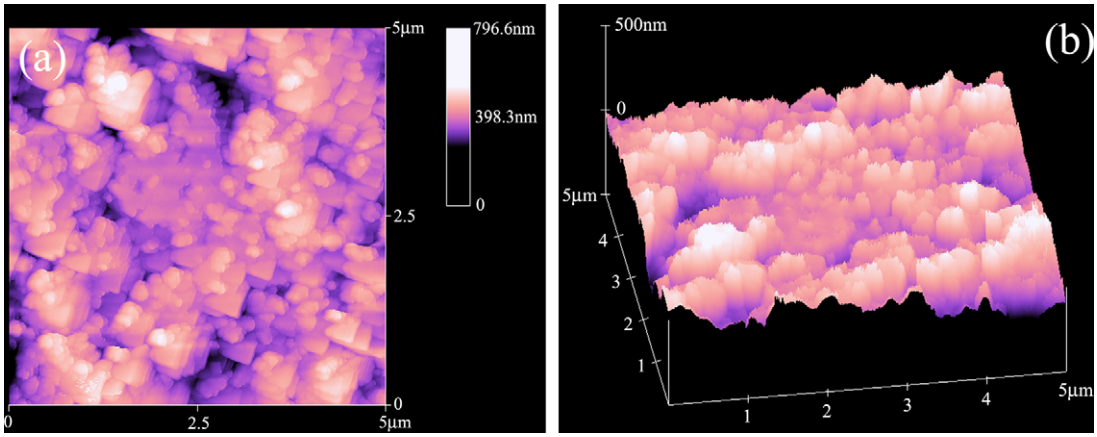

Fig. 4. Planar AFM image (a) and 3D AFM image of the $MgFe_2O_4$ film (b).

The morphology and roughness of $MgFe_2O_4$ film were further characterized by atomic force microscopy. The protrusions and pitches from several tens of nm to hundreds of nm are easily observed in the AFM images (Fig. 4a and b), indicative of the porous nature of the film. The root-mean-square (RMS) roughness and the ratio of actual to projected surface areas (S/S_o) of the film are estimated to be 49.3 nm and 1.368, respectively, suggesting a relatively rough surface.

The field dependence of magnetization for calcined MgFe-LDH and $MgFe_2O_4$ films was measured at room temperature (Fig. 5). The saturation magnetization (M_s) value of calcined MgFe-LDH film is as small as 10.3 emu/g, due to the presence of non-magnetic MgO phase. The M_s value of $MgFe_2O_4$ film reaches 37.1 emu/g, which is apparently larger than that of $MgFe_2O_4$ powder material synthesized by a conventional solid-state method (c.a. 26.4 emu/g) [18]. This could be ascribed to the structural correlations between LDH precursor and its spinel counterpart via a topologic transformation. The 2D layered structure of LDH transforms into 3D structure consisting of a regular oxygen cubic close packed network with a disordered cationic distribution in the interstices upon stepwise heating [20]. In the case of film, the interplays among particles within $MgFe_2O_4$ film lead to the increment of interparticle exchange interactions and thus the enhancement of magnetization [20]. This is consistent with our previous findings of ferrite nanoparticles [18]. On the other hand, it can be observed that the coercivity (H_c) exists in the calcined MgFe-LDH film (Fig. 5a). This can be attributed to non-magnetic MgO as diluted matrix, resulting in the increase of H_c [21].

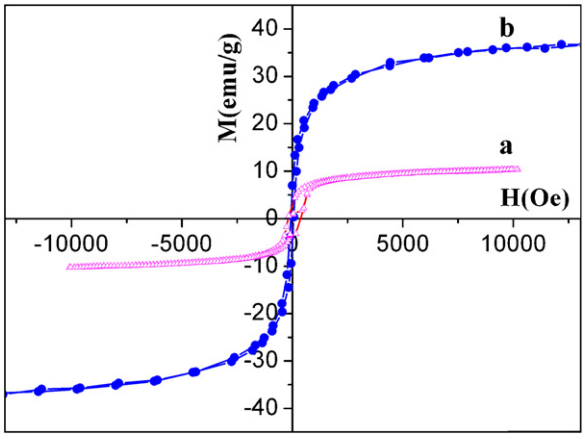

Fig. 5. Magnetization hysteresis loops of calcined MgFe-LDH film before (a) and after (b) the removal of MgO.

The temperature-dependent magnetization of $MgFe_2O_4$ film was studied by a superconducting quantum interference device magnetometer. Fig. 6a shows zero-field cooled and field cooled (FC) curves of the sample within the temperature range from 5 to 300 K. The magnetization gradually increases with the rise of temperature above 5 K until a maximum at 105 K in the ZFC curve, i.e., blocking temperature (T_B = 105 K), at which ZFC and FC curves are bifurcated. The free rotation of magnetic moments is blocked

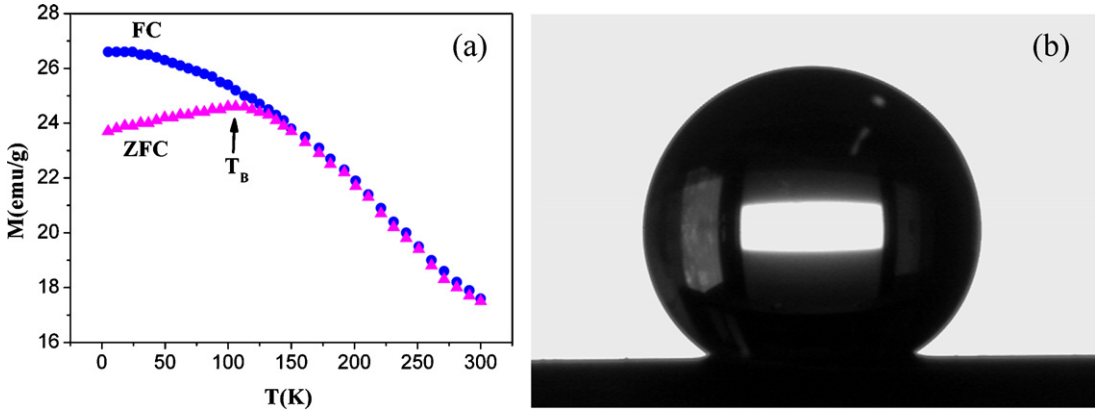

Fig. 6. Temperature-dependent magnetization of $MgFe_2O_4$ film in the ZFC and FC mode with an applied magnetic field of 100 Oe (a) and shape of water droplet on the surface of modified $MgFe_2O_4$ film (b).

by anisotropy below T_B. Above T_B, the thermal energy becomes sufficient enough to make the moment free and thus the system become superparamagnetic. The correlation between the blocking temperature and nanoparticle sizes for $MgFe_2O_4$ powder has been studied [22]. It is commonly believed that superparamagnetic characteristics are related to the magnetic particle sizes below a certain single domain value. The blocking temperature observed here can be associated with the crystallite sizes of $MgFe_2O_4$ powder less than 10 nm according to the reported findings [22]. However, the sizes of $MgFe_2O_4$ in the present case seem to be much larger than those behaving superparamagnetic characteristics, as shown in SEM (Fig. 3c). The unusual superparamagnetic property could be attributed to the unique porous microstructure of the film and the aggregate state consisting of many crystalline subunits with much smaller sizes. The particulate film as a whole can be considered as a bulk material consisting of nanoscale structural units, in which grain boundaries and interfaces occupy quite large volume of material. As a result, the magnetic properties are mostly dominated by interactions among grains. The magnetic behaviour cannot simply be explained by the theories for non-interacting particles with reduced sizes, e.g. nanoparticles in form of powder [23]. Although it is expected that the superparamagnetism for $MgFe_2O_4$ observed here is closely associated with porous and fused particulate microstructure based on the above results, the detailed study is still required to state inherent relationships between structure and magnetism.

Water contact angle measurements are applied for analyzing the surface wettability of the $MgFe_2O_4$ film prepared here. Generally, the wettability of solid surfaces is determined by both their chemical compositions and the geometric morphologies of surfaces. Versatile wettability can be achieved by tuning or modification of surface compositions and structures [24]. Superhydrophobic surfaces, usually with a water droplet contact angle higher than 150°, are commonly created through surface roughening and/or the lowering of the surface free energy [25–28]. It is expected that the porous structure for $MgFe_2O_4$ film in this work may lead to particular surface wettability. For achieving the surface hydrophobicity measurement, the $MgFe_2O_4$ film was modified by n-octadecanoic acid (C18 acid) self-assembled monolayer on the surface. The modification of solid surfaces with some organic molecules is a common way for obtaining low-energy surfaces [27,28]. Fig. 6b shows a photo of water droplet shape on the modified $MgFe_2O_4$ film. The water contact angle is measured to be $151 \pm 1°$, indicative of surface superhydrophobicity. Herein, the surface porosity of the synthesized film favours the efficient trapping of a large fraction of air in the interstices or interspaces of particulate structure when a droplet of water is deposited onto the surface on the basis of Cassie and Baxter's model [24,29]. Also, the porous microstructure of $MgFe_2O_4$ film leads to the exposure of more surface oxygen, allowing for more amount of C18 acid having hydrophobic long-chains assembled onto the surface of film. As a result, the combination of air trapping in porous spacing on substrate surface and lowering of surface energy results in such novel superhydrophobic property.

4. Conclusions

In this article, a new methodology was established to synthesize $MgFe_2O_4$ film based on a precursor synthesis route. The strategy leads to a unique porous and particulate ferrite film from MgFe-LDH precursor due to the removal of self-generated MgO phase. The as-formed $MgFe_2O_4$ film exhibited enhanced magnetization and superparamagnetic characteristics, which are closely correlated with the unique microstructure. Wettability measurements indicate the film modified with organic molecules presents excellent superhydrophobicity. The method established here is a universal one and can easily be extended to other porous ferrite films of technological importance such as Ni-, Zn-, Mn-, Cu-ferrites by simply adjusting the cationic types of precursors. Such significant magnetic and interfacial properties of the film, which never were reported previously, can open up new opportunities for potential applications in magnetic microdevices or anti-wetting surface coatings.

Acknowledgements

We gratefully thank the financial support from the National Natural Science Foundation of China, 973 Program (2009CB939802), 111 Project (No. B07004) and Changjiang Scholars and Innovative Research Team in Universities (IRT 0406).

References

[1] Z.L. Wang, Y. Liu, Z. Zhang, Handbook of Nanophase and Nanostructured Materials, vol. 3, Kluwer Academic/Plenum Publishers, New York, 2002.
[2] J. Park, J. Joo, S. Kwon, Y. Jang, T. Hyeon, Angew. Chem. Int. Ed. 46 (2007) 4630–4660.
[3] C. Bárcena, A.K. Sra, G.S. Chaubey, C. Khemtong, J.P. Liu, J. Gao, Chem. Commun. (2008) 2224–2226.
[4] T. Bala, C.R. Sankar, M. Baidakova, V. Osipov, T. Enoki, P.A. Joy, B.L.V. Prasad, M. Sastry, Langmuir 21 (2005) 10638–10643.
[5] S. Bhattacharyya, J.-P. Salvetat, R. Fleurier, A. Husmann, T. Cacciaguerra, M.-L. Saboungi, Chem. Commun. (2005) 4818–4820.
[6] N. Bao, L. Shen, Y. Wang, P. Padhan, A. Gupta, J. Am. Chem. Soc. 129 (2007) 12374–12375.
[7] Y. Huang, Y. Tang, J. Wang, Q. Chen, Mater. Chem. Phys. 97 (2006) 394–397.
[8] A.-K. Axelsson, M. Valant, L. Fenner, A.S. Wills, N.M. Alford, Thin Solid Films 517 (2009) 3742–3747.
[9] V. Šepelák, A. Feldhoff, P. Heitjans, F. Krumeich, D. Menzel, F.J. Litter, I. Bergmann, K.D. Becker, Chem. Mater. 18 (2006) 3057–3067.
[10] P.S. Braterman, Z.P. Xu, F. Yarberry, in: S.M. Auerbach, K.A. Carrado, P.K. Dutta (Eds.), Handbook of Layered Materials, Marcel Dekker, New York, 2004, pp. 373–474, (Chapter 8).
[11] D.G. Evans, R.C.T. Slade, Struct. Bonding 119 (2006) 1–87.
[12] F. Zhang, X. Xiang, F. Li, X. Duan, Catal. Surv. Asia 12 (2008) 253–265.
[13] D.G. Evans, X. Duan, Chem. Commun. (2006) 485–496.
[14] H. Chen, F. Zhang, S. Fu, X. Duan, Adv. Mater. 18 (2006) 3089–3093.
[15] F. Zhang, L. Zhao, H. Chen, S. Xu, D.G. Evans, X. Duan, Angew. Chem. Int. Ed. 47 (2008) 2466–2469.
[16] M. Bellotto, B. Rebours, O. Clause, J. Lynch, D. Bazin, E. Elkaim, J. Phys. Chem. 100 (1996) 8535–8542.
[17] J. Liu, F. Li, D.G. Evans, X. Duan, Chem. Commun. (2003) 542–543.
[18] F. Li, J. Liu, D.G. Evans, X. Duan, Chem. Mater. 16 (2004) 1597–1602.
[19] L. Zou, X. Xiang, J. Fan, F. Li, Chem. Mater. 19 (2007) 6518–6527.
[20] R.D. Zysler, D. Fiorani, A.M. Testa, J. Magn. Magn. Mater. 224 (2001) 5–11.
[21] T. Yang, C. Shen, Z. Li, H. Zhang, C. Xiao, S. Chen, Z. Xu, D. Shi, J. Li, H. Gao, J. Phys. Chem. B 109 (2005) 23233–23236.
[22] C. Liu, B. Zou, A.J. Rondinone, Z.J. Zhang, J. Am. Chem. Soc. 122 (2000) 6263–6267.
[23] D.L. Leslie-Pelecky, R.D. Rieke, Chem. Mater. 8 (1996) 1770–1783.
[24] X.J. Feng, L. Jiang, Adv. Mater. 18 (2006) 3063–3068.
[25] Q. Xie, J. Xu, L. Feng, L. Jiang, W. Tang, X. Luo, C.C. Han, Adv. Mater. 16 (2004) 302–305.
[26] S. Li, H. Li, X. Wang, Y. Song, Y. Liu, L. Jiang, D. Zhu, J. Phys. Chem. B 106 (2002) 9274–9276.
[27] Y. Li, X.J. Huang, S.H. Heo, C.C. Li, Y.K. Choi, W.P. Cai, S.O. Cho, Langmuir 23 (2007) 2169–2174.
[28] Z. Guo, F. Zhou, J. Hao, W. Liu, J. Am. Chem. Soc. 127 (2005) 15670–15671.
[29] A.B.D. Cassie, S. Baxter, Trans. Faraday Soc. 40 (1944) 546–551.